Title
Open loop optogenetic control of simulated cortical epileptiform activity

Authors
Selvaraj, Prashanth
Sleigh, Jamie W.
Freeman, Walter J.
et al.

Publication Date
2014-06-03

Peer reviewed

Journal of Computational Neuroscience manuscript No.
(will be inserted by the editor)

Open loop optogenetic control of simulated cortical epileptiform activity

Prashanth Selvaraj · Jamie W. Sleigh · Walter J. Freeman · Heidi E. Kirsch · Andrew J. Szeri

Received: date / Accepted: date

Abstract We present a model for the use of open loop optogenetic control to inhibit epileptiform activity in a meso scale model of the human cortex. The meso scale cortical model first developed by [11] is extended to two dimensions and the nature of the seizure waves is studied. We adapt to the meso scale a 4 state functional model of Channelrhodopsin-2 (ChR2) ion channels. The effects of pulsed and constant illumination on the conductance of these ion channels is presented. The inhibitory cell population is targeted for the application of open loop control. Seizure waves are successfully suppressed and the inherent properties of the optogenetic channels ensures charge balance in the cortex, protecting it from damage.

Keywords Meso-scale cortical model · Seizure propagation · Optogenetic control

1 Introduction

About 70% of people suffering from epileptic seizures can be treated with anti-epileptic drugs (AEDs). For the remaining 30% with medically refractory, more commonly focal-onset, epilepsy, surgical removal of the epileptogenic zone is a treatment option, as are implanted neurostimulators such as the vagal nerve stimulator. Options on the horizon include closed-loop devices that sense the onset of a seizure and deliver local therapy to interrupt the seizure's spread. For example, the firing pattern of neurons bear the epileptogenic zone can be altered by changing their mean soma potential by the application of an external electric field. *In vitro* experiments on rat cortex [15] showed it is possible to modulate the behaviour of seizure like waves, while *in vivo* experiments on rats [5] showed that stimulation using proportional feedback temporarily inhibited seizure waves. Electrical cortical stimulation was modelled computationally [8] using various methods of feedback control and charge balanced control was ensured in subsequent work [12]. Here, we present another method of suppressing seizure waves by altering the mean soma potential of cells via the use of optogenetic channels.

The use of light as an input signal to stimulate neurons was first suggested in 1999 by Sir Francis Crick [3]. Since then the field of optogenetics has come a long way, being named 'Method of the year' in 2010 [4]. Optogenetics uses photoreceptors which are genetically targeted onto cells of interest. When illuminated with light of a certain wavelength, optogenetic ion channels facilitate a transfer of cations or anions between the cell and the extra-cellular region. Two of the most popular optogenetic channels are channelrhodopsin-2 (ChR2), which is a cation pump introduced in 2004 [13], and *Natromonas pharaonis* halorhodopsin (NpHR), which is a chloride pump introduced in 2007 [19].

The control of seizures using closed loop optogenetic control has been demonstrated in rats [17, 14] and in mice [10], where hyperpolarising excitatory neurons or depolarising inhibitory neurons in the hippocampus or the thalamus leads to the suppression of seizure waves. In this work, we present a method of seizure suppression where we depolarise the inhibitory cells in a model of the human cortex using ChR2 channels. The firing of the inhibitory cells suppresses the firing of excitatory cells, and this subsequently leads to the disruption of pathological synchronous firing of cortical neurons.

This paper is organised as follows. First, we present the meso scale model of the cortex, and how it may be used to model the origin and propagation of seizure

Prashanth Selvaraj
University of California, Berkeley
Berkeley, CA 94704 E-mail: pselvaraj@me.berkeley.edu

waves. Next, we adapt to the meso scale a model of the dynamics of ChR2 channels in the cortex, and their behaviour when illuminated with either constant or pulsed light is studied. Finally, we present results from the use of ChR2 channels on inhibitory cells to implement open loop control.

2 2D cortical model

To simulate electrical activity in the human cortex ideally, one would have to model the connections between individual neurons taking into account the characteristics of each neuron (location, connections to other neurons, pyramidal or stellate etc.). However, given the limits of computing capacity, it would be extremely difficult to model a network consisting of all of these neurons even if the complicated physiology were well defined. To avoid this, we use the meso scale model of the human cortex developed by [11] that is characterised by a set of 8 non-linear stochastic partial differential equations (SPDEs). The mathematical model is written in the following way:

$$\frac{\partial \tilde{h}_e}{\partial \tilde{t}} = 1 - \tilde{h}_e + \Gamma_e(h_e^0 - \tilde{h}_e)\tilde{I}_{ee} + \Gamma_i(h_i^0 - \tilde{h}_e)\tilde{I}_{ie} \tag{1}$$

$$\frac{\partial \tilde{h}_i}{\partial \tilde{t}} = 1 - \tilde{h}_i + \Gamma_e(h_e^0 - \tilde{h}_i)\tilde{I}_{ei} + \Gamma_i(h_i^0 - \tilde{h}_i)\tilde{I}_{ii} \tag{2}$$

$$\left(\frac{1}{T_e}\frac{\partial}{\partial \tilde{t}} + 1\right)^2 \tilde{I}_{ee} = N_e^\beta \tilde{S}_e\left[\tilde{h}_e\right] + \tilde{\phi}_e + P_{ee} + \tilde{\Gamma}_1 \tag{3}$$

$$\left(\frac{1}{T_e}\frac{\partial}{\partial \tilde{t}} + 1\right)^2 \tilde{I}_{ei} = N_e^\beta \tilde{S}_e\left[\tilde{h}_e\right] + \tilde{\phi}_i + P_{ei} + \tilde{\Gamma}_2 \tag{4}$$

$$\left(\frac{1}{T_e}\frac{\partial}{\partial \tilde{t}} + 1\right)^2 \tilde{I}_{ie} = N_i^\beta \tilde{S}_i\left[\tilde{h}_i\right] + P_{ie} + \tilde{\Gamma}_3 \tag{5}$$

$$\left(\frac{1}{T_e}\frac{\partial}{\partial \tilde{t}} + 1\right)^2 \tilde{I}_{ii} = N_i^\beta \tilde{S}_i\left[\tilde{h}_i\right] + P_{ii} + \tilde{\Gamma}_4 \tag{6}$$

$$\left(\frac{1}{\lambda_e}\frac{\partial}{\partial \tilde{t}} + 1\right)^2 \tilde{\phi}_e = \frac{1}{\lambda_e^2}\nabla^2\tilde{\phi}_e + \left(\frac{1}{\lambda_e}\frac{\partial}{\partial \tilde{t}} + 1\right) N_e^\alpha \tilde{S}_e\left[\tilde{h}_e\right] \tag{7}$$

$$\left(\frac{1}{\lambda_i}\frac{\partial}{\partial \tilde{t}} + 1\right)^2 \tilde{\phi}_i = \frac{1}{\lambda_i^2}\nabla^2\tilde{\phi}_i + \left(\frac{1}{\lambda_i}\frac{\partial}{\partial \tilde{t}} + 1\right) N_i^\alpha \tilde{S}_e\left[\tilde{h}_e\right] \tag{8}$$

Here, all variables have been non dimensionalised and are functions of time $\tilde{t}$, and the two spatial dimensions $\tilde{x}$ and $\tilde{y}$. The subscripts e and i represent excitatory and inhibitory populations respectively, and variables with two subscripts represent the transfer of energy from one population to another. The mean soma potential for a neuronal population is represented by the $\tilde{h}$ state variable, $\tilde{I}$ represents the postsynaptic activation due to local, long-range, and subcortical inputs. $\tilde{\phi}$ represents long range (corticocortical) inputs. Values and explanations for all parameters and variables can be obtained from [9].

This model and EEG or ECoG data from a patient undergoing seizure are in good agreement on the average frequency of maximum power and the speed of spatial propagation of voltage peaks [9]. Also, the variables of the mean field model are spatially averaged properties of neuron populations, and can be related to EEG and ECoG measurements which represent the spatially averaged extracellular local field potential (LFP). The sign reversed LFP, in turn, is proportional to the spatially averaged excitatory soma membrane potential, h_e, which is one of the variables used in the SPDEs. It has been shown that increasing the subcortical input results in h_e mimicking ECoG data obtained from a seizing cortex [9]. Here, we look at tonic-clonic seizures characterised by runaway excitation, and this makes the meso scale model ideal for this study.

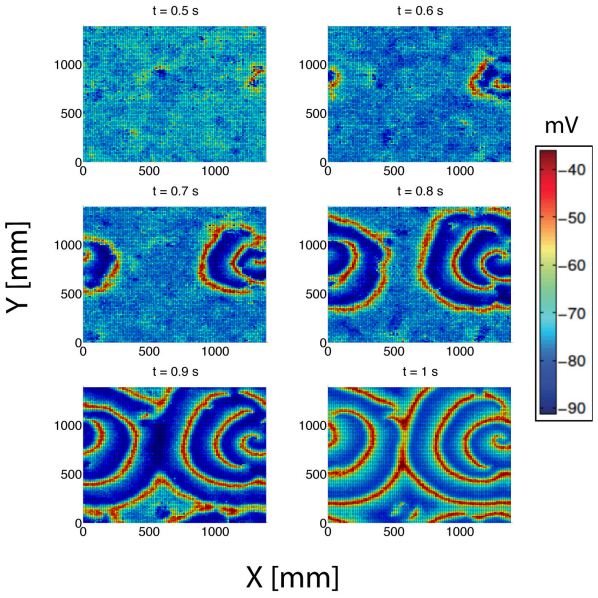

Fig. 1: Propagation of seizure waves in a 2D model of cortex which measure $1400 \times 1400\ mm^2$. Snapshots taken from time t = $0.5s$ to t = $1s$. Stochastic fluctuating inputs readily trigger a seizure wave when the model cortex is put in a state susceptible to seizures, which is characterized here by the baseline parameters of [9] for normal cortical function, except for $P_{ee} = 548.0$ and $\Gamma_e = 0.8 \times 10^{-3}$.

The evolution and propagation of seizure waves in a one dimensional cortical model has been shown in previous work [12] and [9]. The 1D model has been extended to a 2D model by using the two dimensional Laplacian ($\partial^2/\partial x^2 + \partial^2/\partial y^2$) instead of just one sec-

ond order spatial derivative, leading to the long range connections scaled by a spatial decay in two dimensions. Fig.(1) depicts an example, showing the propagation of seizure waves in a two dimensional cortex of size 1400 mm $\times$ 1400 mm.[1] Seizure waves originate at a focus in response to stochastic fluctuations and propagate outwards in spiral waves. This is in good agreement with the results for the multi neuron integrate and fire network model in [18]. Fig. 2a shows the variation of the mean soma potential of the excitatory cell population at a point in the cortex. The cortex starts exhibiting synchronous behaviour at around 0.2s. Fig. 2b shows travelling seizure waves in a 1D slice of the 2D model cortex.

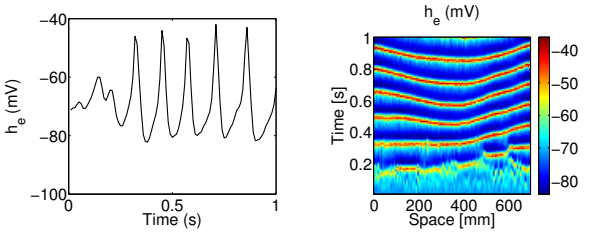

(a) At a point in the domain (b) 1D slice of the 2D domain

Fig. 2: Seizure wave propagation in a two dimensional meso scale model of the human cortex, with $P_{ee} = 548.0$, $\Gamma_e = 0.66 \times 10^{-3}$ and $\alpha = 1$. The model cortex measures 700×700 mm^2. The colour bar shows mean soma potential values in mV.

3 Meso scale optogenetics model

The meso scale optogenetics model described here is based on the four state model of Channelrhodopsin-2 (ChR2) cells first proposed by [13]. This model was able to reproduce qualitatively the ChR2 photocurrents obtained from experimental measurements. It takes into account the fact that the recovery rates under constant illumination and in the dark are different and is thus able to simulate the characteristic peak-plateau behaviour and degraded transient response for subsequent stimulus. Building on this and a ChR1 model [7], a 4 state model for ChR2 channels was proposed and the effect of the change in conductance on a neuron described by a cable model, which contains active HodgkinHuxley type elements, was studied [6].

[1] The average human cortex has dimensions of 500×500 mm^2 if it were laid open like a sheet. However, the spiral seizure waves have a radius of curvature that is too large to be appreciated within a domain of the size of an average human cortex, and because cortical dynamics is scale-free, we have used a larger cortical domain to illustrate them.

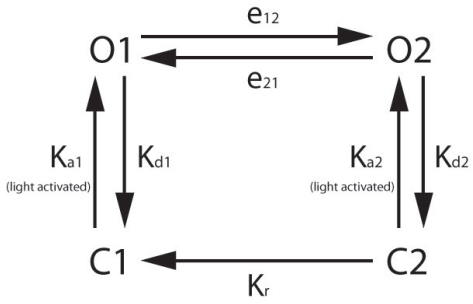

Fig. 3: Transition from one optogenetic state to another in the 4 state model for ChR2 channels.

The 4 state model has two open states ($O1$ and $O2$) and two closed states ($C1$ and $C2$). These states do not actually represent the physical energy levels of ChR2, but instead describe a functional model that is a good representation of the behaviour of ChR2 ion channels when illuminated with light. The conductivity in the $O1$ state is more than in the $O2$ state, but the $O2$ state has a longer life time. Conversion from one state to the other can be achieved through both light and thermal excitation. Fig.(3) illustrates the possible transitions from one state to another. The equations describing the 4 state model are based on those of [6].

$$\frac{dN_{O1}}{dt} = K_{a1}.N_{C1} - (K_{d1} + e_{12}).N_{O1} + e_{21}.N_{O2} \tag{9}$$

$$\frac{dN_{O2}}{dt} = K_{a2}.N_{C2} + e_{12}.N_{O1} + (K_{d2} + e_{21}).N_{O2} \tag{10}$$

$$\frac{dN_{C2}}{dt} = K_{d2}.N_{O2} - (K_{a2} + K_r).N_{C2}, \tag{11}$$

Equations 9-11 describe the number of channels in each open and closed state, represented by N_{Oi} and N_{Ci} respectively. K_{ai} are the rates of transition from the closed states, $C1$ and $C2$, to the open states $O1$ and $O2$ respectively. Conversely, K_{di} are the closing rates from the open states to the closed states. K_r is the thermal recovery rate from $C2$ to $C1$. e_{12} and e_{21} are the transition rates from $O1$ to $O2$ and vice versa. The values for all rate constants can be found in table 1.

This optogenetic model was originally developed to study the effect of optogenetic conductance on a cable model of a neuron with active Hodgkin-Huxley type elements [6]. The computational domain for our meso scale cortical model is broken up into 100×100 cells which corresponds to a total area of 700×700 mm^2. To adapt the optogenetic model to the meso scale, the values of N_{Oi} and N_{Ci} have been normalised with the total number of ChR2 channels per representative neuron, and now represent the fraction of channels in each state

Table 1: Rate constant values for the meso scale optogenetic model of ChR2 embedded in the cortex.

Rate constant	Transition from	Value (ms^{-1})
K_{a1},K_{a2}	C1 to O1, C2 to O2	0.5Φ, 0.12Φ
K_{d1},K_{d2}	O1 to C1, O2 to C2	0.1, 0.5
e_{12},e_{21}	O1 to O2, O2 to O1	$.011+.005log(\Phi/0.024)$, $0.008+0.004log(\Phi/0.024)$
K_r	C2 to C1	$1/3000$

$\Phi(t)$ is the photon flux per ChR2 and has units of ms^{-1}. K_{ai} is given by the quantum efficiency times the photon flux, $\varepsilon_i.\Phi(t)$.

per representative neuron. The sum of these fractions equals unity, and is described in eq.12.

$$N_{O1}+N_{O2}+N_{C1}+N_{C2}=1. \quad (12)$$

By multiplying these fractions with the expression density (ion channels per unit area of cell membrane) and the area of each representative neuron, we obtain the total number of ion channels per representative neuron, and consequently, the total conductance of all the ion channels per representative neuron. It should be noted that while we are dealing with chemical dynamics at the molecular scale to describe the state of optogenetic channels, it is reasonable to scale the idea up to the meso scale that describes the cortex because the cortical model represents a population of spatially averaged neurons.

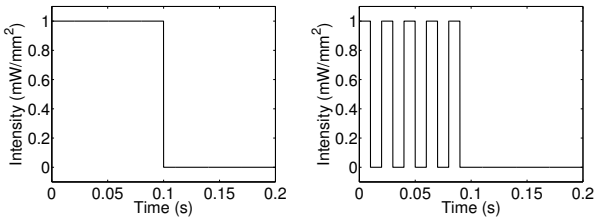

Fig. 4: Constant and pulsed illumination profiles for light intensity of 1 mW/mm^2.

In this study, we have not taken into account the light cone [2] emitted by each light source and the variation in illumination intensity they produce over a given area. Instead, we model the average intensity throughout a representative neuron with no overlap between two light cones. Fig. 4 shows the two kinds of illumination profiles we use for optogenetic actuation, and fig. 5 depicts the corresponding optogenetic conductance for a given illumination using a constant cell membrane voltage of $-70\ mV$. For both constant and pulsed illumination, light intensities of 1 mW/mm^2, 0.1 mW/mm^2 and 0.01 mW/mm^2 have been used. The pulsing of light has a markedly different effect on a cortical model without a voltage clamp, and this is demonstrated in the next section. Here, we use a fourth order Runge Kutta method to solve equations 9-11.

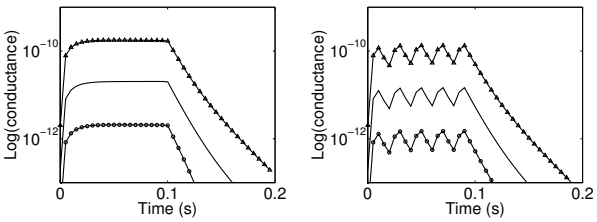

(a) Constant illumination (b) Pulsed Illumination

Fig. 5: Semi-log plot showing variation of conductance with light intensity for an ion channel density of 10^9ChR2's/m^2. △− - 1 mW/mm^2, − - 0.100 mW/mm^2, •− - 0.01 mW/mm^2. If the conductance were multiplied by the clamped voltage value of -70 mV, it would reproduce the plot of current vs. time in [6].

Fig. 5a shows the difference between the conductance of optogenetic channels illuminated by 1 mW/mm^2, 0.1 mW/mm^2 and 0.01 mW/mm^2 light intensities. The peak to plateau ratio of the conductance is decreased and intensity decreases. Also, the peak and plateau values decrease as the intensity is decreased. Similar behaviour is observed in the case with pulsed illumination. Fig. 5b shows the conductance has sharper spikes when a lower intensity is used. However, with a higher intensity, the peak conductance value decreases less rapidly at the highest point before dropping off again when the light is turned off. Both constant and pulsed illumination profiles produce a sharp rise in conductance value before it reaches a steady state after about 50 ms.

4 Open loop control

We now introduce open loop control using optogenetic ion channels.

$$\frac{\partial \tilde{h}_i}{\partial \tilde{t}} = 1-\tilde{h}_i+\Gamma_e(h_e^0-\tilde{h}_i)\tilde{I}_{ei}+\Gamma_i(h_i^0-\tilde{h}_i)\tilde{I}_{ii}-u, \quad (13)$$

is a modification of eqn. 2 that includes the control term u. ChR2 channels are cation pumps that conduct Na^+, Ca^{2+} , H^+ and K^+ ions.

The control term is defined as

$$u = h_i.G_{ChR2}.R_m. \quad (14)$$

This formulation is dependent on the mean soma potential of the inhibitory population, and the mean membrane resistance of these cells represented by R_m is obtained from voltage clamp experiments and has a value of $7.1G\Omega$[16]. The conductance of ChR2 channels is given by,

$$G_{ChR2} = G_{max}.g_{ChR2}.\frac{(1-exp(-h_i/U_0))}{h_i/U_1}.N_{ChR2}, \quad (15)$$

where h_i is the membrane potential for the inhibitory population, G_{max} is the maximum conductance of optogenetic channels in the $O1$ state, g_{ChR2} is the total conductance of the optogenetic channels in the $O1$ and $O2$ states defined by $(g_{O1}.N_{O1} + g_{O2}.N_{O2})$. U_0 and U_1 are empirical constants with values of $40mV$ and $15mV$ respectively. N_{ChR2} is the number of ChR2 channels per cortical macrocolumn.

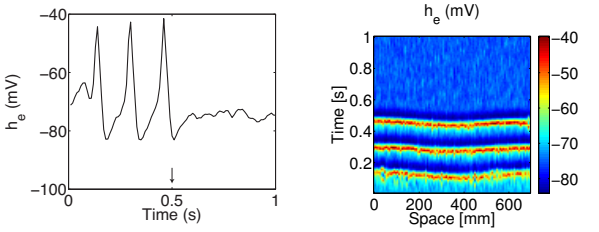

(a) At a point in the domain (b) 1D slice of the 2D domain

Fig. 6: Optogenetic seizure control using constant illumination of intensity 20 mW/mm^2. The model cortex measures 700×700 mm^2, with $P_{ee} = 548.0$, $\Gamma_e = 0.66 \times 10^{-3}$ and $\alpha = 1.15$. The arrow in fig. 6a indicates control being turned on at 0.5s. The colour bar shows mean soma potential values in mV.

In what follows, the use of optogenetic channels to inhibit seizure waves is illustrated. Control is actuated at 0.5s by illuminating the cortex with light of 470 nm. From eq. 15 it can be seen that the net conductance produced for a given light intensity is directly proportional to the number of ChR2 channels expressed. Here, we have used a channel expression density (number of ChR2 channels per unit area) of $\sim 10^9/\mathrm{m}^2$ in order to use illumination intensities that correspond to experiments [2]. Fig. 6 uses a constant light intensity source of 20 mW/mm^2 to illuminate the cortex, while fig. 7 uses a pulsed light source of 40 mW/mm^2. Both plots are of the mean soma potential of the excitatory population.

The time scale at which the dynamics of the meso scale cortex occur is larger than the time scale of the optogenetic channel dynamics. We used a two step predictor corrector numerical method to solve the set of SPDEs, and a first order forward Euler method to solve the optogenetic ODEs at each point in the domain. [2]

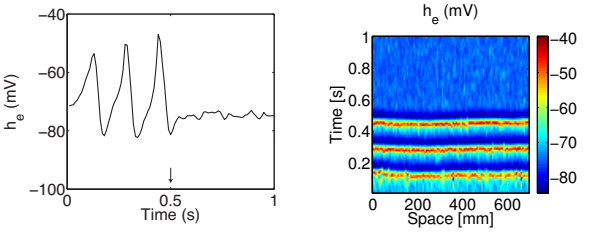

(a) At a point in the domain (b) 1D slice of the 2D domain

Fig. 7: Optogenetic seizure control using pulsed illumination of intensity 40 mW/mm^2 with 0.005s pulses. The model cortex measures 700×700 mm^2, with $P_{ee} = 548.0$, $\Gamma_e = 0.66 \times 10^{-3}$ and $\alpha = 1.15$. The arrow in fig. 7a indicates control being turned on at 0.5s. The colour bar shows mean soma potential values in mV.

The mechanism for seizure control using this approach is as follows. When ChR2 that is expressed in the inhibitory cell population is activated with light, it pumps cations from the extra-cellular space into the inhibitory cells, and this depolarises them. This changes the mean soma potential and the firing rate of the inhibitory population, which in turn changes the mean soma potential of the excitatory population through the influence of the postsynaptic activation due to the inhibitory population ($\tilde{I}_{ie}$). The firing rate of a representative neuron is determined by its mean soma potential, so by changing the mean soma potential, the firing rate can be changed as well. The seizures discussed

[2] The fourth order solver is more accurate in producing results that match experimental observations of conductance, but the first order method takes less computation time to solve the equations. Because the optogenetic channels function at a smaller time scale, and because we are only interested in time scales of the cortical model, the use of the simpler first order method is justified.

here are caused by runaway excitation, so by increasing the firing rate of the inhibitory population the firing rate of excitatory cells, which fire synchronously during epileptic seizures, can be inhibited, breaking the synchronicity and inhibiting seizure waves.

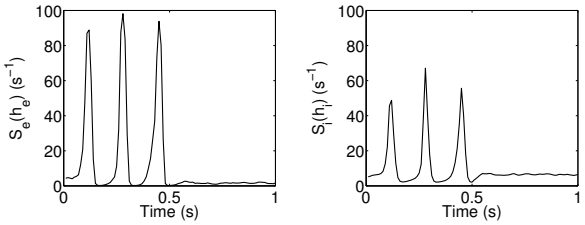

(a) Excitatory population (b) Inhibitory population

Fig. 8: Firing rates for the excitatory and inhibitory population with optogenetic control applied at 0.5s

Fig. 8, shows how the baseline value of firing rate for the inhibitory population is higher than that of the excitatory population after optogenetic control is applied at 0.5s. It should be noted here that Fig. 8 depicts the firing rate of a representative neuron in the mean field model, and not the spiking of an individual neuron.

4.1 Pulsed Illumination

Optogenetic control using pulsed illumination depends on the intensity and the pulsing profile. In figures 9 and 10 we use two different pulsing profiles with the same peak intensity used to generate 7, where a 0.005s pulse was used.

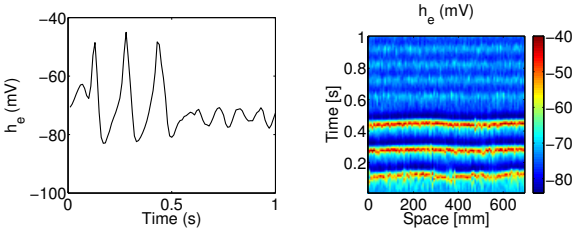

(a) Mean soma potential at a point (b) 1D slice of a 2D domain

Fig. 9: Optogenetic control applied at 0.5s using 0.05s pulsed illumination. Synchronous behaviour persists even after control is applied, but the amplitude of seizure waves is decreased. Parameters: $P_{ee} = 548.0$, $\Gamma_e = 0.00066$, $\alpha = 1.15$, expression density $= 10^4$ ChR2s/m^2, Intensity $= 40$ mW/mm^2.

Fig. 9 was generated using light pulses of 0.05s duration. While the amplitude of the seizure waves is decreased considerably, it is seen that synchronous behaviour persists despite control being applied at 0.5s. This is because the dark regions of the pulsing profile, where the ion channels tend to close, is long enough to reduce control to a low value where it does not have a considerable effect on the seizing cortex. However, the frequency of the pulsing still ensures the oscillations are not fully developed because control does not go to zero during the dark regions.

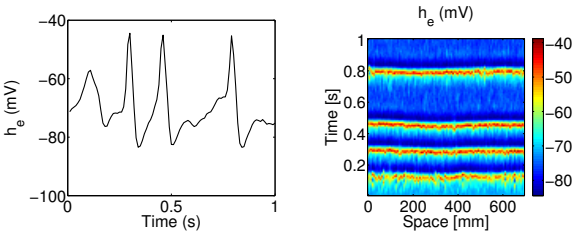

(a) Mean soma potential at a point (b) 1D slice of a 2D domain

Fig. 10: Pulsed optogenetic control using 0.08s pulses applied at 0.5s. Frequency of seizure waves has decreased, but amplitude of oscillations is invariant. Parameters: $P_{ee} = 548.0$, $\Gamma_e = 0.00066$, $\alpha = 1.15$, expression density $= 10^4$ ChR2s/m^2, Intensity $=$ 40 mW/mm^2 - pulsed illumination with 0.08 s pulses.

In fig. 10 light pulses of 0.08s duration were used. In this case, seizure waves have not been inhibited, but the frequency has been reduced. This can be accounted for by the duration of the dark periods of pulsing which is long enough to close the ion channels completely leading to zero control. During the dark period, the cortex starts seizing again, but the seizures are inhibited completely during the illuminated periods of pulsing. Finally, using 0.0005s pulses we successfully break down all synchronous behaviour and inhibit seizure waves in fig. 7. With the shorter pulses the dark periods aren't long enough for most of the optogenetic channels to close and this results in behaviour similar to constant illumination where the majority of the channels are open.

5 Robustness of control

In this section we explore the robustness of the control approach to changes in different aspects of the model. The parameters for the meso scale model are varied within ranges provided in [1] and [11].

5.1 Stochastic inputs

The subcortical input contributes to the postsynaptic activation through constant P_{ij} and stochastic inputs defined by

$$\tilde{\Gamma} = \alpha\sqrt{P_{ij}}\xi[\tilde{x},\tilde{t}]$$

where α is a scaling parameter for the stochastic inputs and ξ is zero mean, Gaussian white noise in time and space.

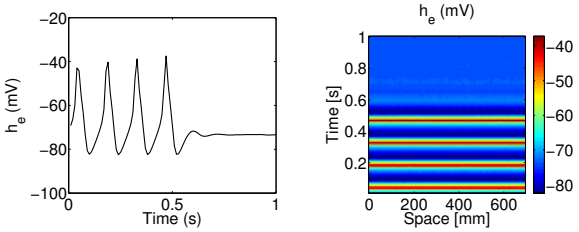

(a) Mean soma potential at a point (b) 1D slice of a 2D domain

Fig. 11: More uniform seizures produced with low noise. Control switched on at 0.5s successfully inhibiting seizures. Parameters: $\alpha = 0.05$, $\Gamma_e = 0.0008$, $P_{ee} = 548.0$, expression density $= 10^4$ ChR2s/m^2, Intensity $= 40$ mW/mm^2 - constant illumination.

Figures 6, 11 and 12 demonstrate the efficacy of the optogenetic control method for different stochastic inputs over two orders of magnitude of noise. Seizure waves are successfully inhibited for α values of 0.05, 1.15 and 5, using the same expression density and constant illumination for all three cases.

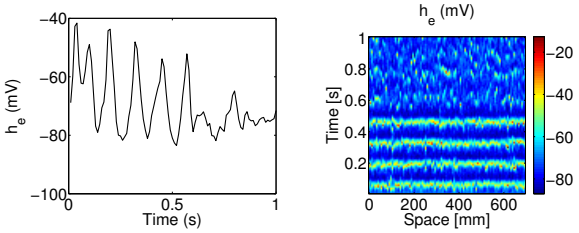

(a) Mean soma potential at a point (b) 1D slice of a 2D domain

Fig. 12: Higher α causes noisier oscillations, however, control is still successful in diminishing synchronous activity when applied at 0.5s. Parameters: $\alpha = 5$, $\Gamma_e = 0.00066$, $P_{ee} = 548.0$, expression density $= 10^4$ ChR2s/m^2, Intensity $= 60$ mW/mm^2 - constant illumination.

5.2 Seizure hotspot

While the cortex has been laid out like a sheet in our figures, it is made up of a number of folds in reality. When optogenetic channels are expressed in the cortex, the ones on the gyri have a better chance of being illuminated.

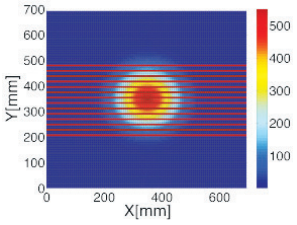

Fig. 13: Gaussian distribution of P_{ee} (seizure hotspot) with a gyri to sulci area ratio of 1:2. Red lines running across the model cortex represent gyri populated with optogenetic channels.

In order to account for this reduction in the number of channels being illuminated, fig. 14 only has channels expressed in a third of the cortical surface area. The sites of optogenetic expression are in strips running across the cortex (representing gyri) separated by strips of zero optogenetic channel expression (representing sulci). We have also included a seizure hotspot by using a Gaussian distribution for P_{ee} with a maximum value of 548.0. Seizure waves arise where the value of P_{ee} is high enough and travel outward until the level of excitation is too low to support them. It should also be noted that the channel expression only covers the hotspot area of the model cortex as shown in fig. 13.

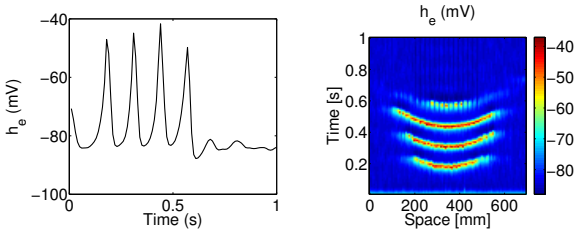

(a) Mean soma potential at a point (b) 1D slice of a 2D domain

Fig. 14: Seizure hotspot with maximum P_{ee} at the center of the model cortex. with a gyri to sulci ratio of 1:2. Parameters: $P_{ee} = 548.0$, $\Gamma_e = 0.001$, $\alpha = 1.6$, expression density $= 2 \times 10^4$ ChR2s/m^2, Intensity $=$ 20 mW/mm^2 - constant illumination.

Fig. 14 shows the application of optogenetic control at 0.5s to a cortex that has a gyri to sulci ratio of 1:2. The expression density has been increased by a factor of 2, but the control is successful in inhibiting seizures. As a first attempt to account for the geometry of the cortex and the ability to illuminate it, fig. 14 demonstrates the efficacy of using optogenetics as a control method.

5.3 Changes in cortical model parameters

The parameters of the meso scale model remain constant during our simulations. However, the cortex is more plastic. To account for this plasticity, parameters like the number of long range connections between cell populations and the neurotransmitter rate constants were changed within their physiological bounds [11], and the effect of optogenetic control on the model seizing cortex was studied.

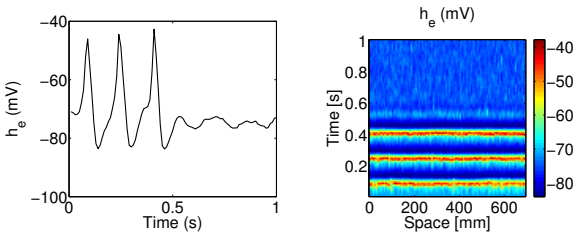

(a) Mean soma potential at a point (b) 1D slice of a 2D domain

Fig. 15: Change in the long range connectivity N_j^α to demonstrate efficacy of the controller when the connectivity is changed . Parameters: $P_{ee} = 548.0$, $\Gamma_e = 0.00066$, $\alpha = 1.15$, expression density $= 10^4$ ChR2s/m^2, Intensity $= 60$ mW/mm^2 - constant illumination, $N_e^\alpha = 5000$, $N_i^\alpha = 3000$.

The long range connections are critical to a seizing cortex [14]. In fig. 15 the number of long range connections from the excitatory cells to other excitatory or inhibitory cells was changed from the normative values of 4000 $e-e$ and 2000 $e-i$, where e and i represent the excitatory and inhibitory populations respectively, to the extrema of their ranges [11]. It is seen that the model cortex can be driven to seizures only if both the $e-e$ and $e-i$ connections are increased. To this end, we used 5000 $e-e$ connections and 3000 $e-i$ connections for our simulations, and the seizing cortex was successfully brought under control using a constant illumination intensity of 60 mW/mm^2.

In figures 16 and 17 the neurotransimtter rate constants T_e and T_i are changed to 20 and 4 respectively

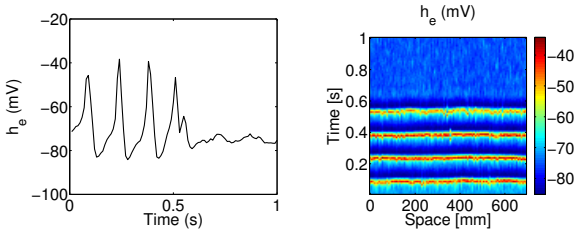

(a) Mean soma potential at a point (b) 1D slice of a 2D domain

Fig. 16: Change in the neurotransmitter rate constant T_e to demonstrate efficacy of the controller when the connectivity is changed . Parameters: $P_{ee} = 548.0$, $\Gamma_e = 0.00066$, $\alpha = 1.15$, expression density $= 10^4$ ChR2s/m^2, Intensity $= 60$ mW/mm^2 - constant illumination, $T_e = 20$, $T_i = 2.6$.

from the normative values of 12 and 2.6. Again, seizures are produced in the cortical model, but they are successfully inhibited when optogenetic control is applied at 0.5s.

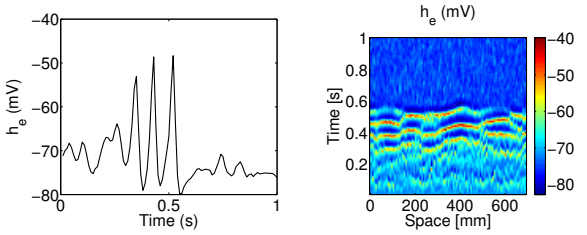

(a) Mean soma potential at a point (b) 1D slice of a 2D domain

Fig. 17: Change in the neurotransmitter rate constant T_i to demonstrate efficacy of the controller when the connectivity is changed . Parameters: $P_{ee} = 548.0$, $\Gamma_e = 0.00066$, $\alpha = 1.15$, expression density $= 10^4$ ChR2s/m^2, Intensity $= 60$ mW/mm^2 - constant illumination, $T_e = 12.0$, $T_i = 4.0$.

6 Conclusion

A method of seizure control using optogenetic channels in a model of the human cortex has been presented. First, the focal origin of seizure waves and their spiral nature was demonstrated. This is in good agreement with the results of [18] multi neuron integrate and fire network model. Then, a meso scale optogenetic model was presented and its light activated characteristics studied. Two illumination profiles were used, constant and pulsed. In a voltage clamped sense, the peak conductance produced by both illumination profiles was

the same. However, while constant illumination saturates at some value after a few milliseconds, pulsed illumination varies at the frequency of the pulsing. Also, the dependence of the total conductance of the optogenetic channels on the light intensity at a point in the cortex shows higher intensities produce higher conductances. However, at a certain intensity, the conductance value plateaus irrespective of the illumination profile used, and this is called the saturation intensity. For the clamped voltage case, the conductance saturates at 160 mW/mm^2.

Open loop control using ChR2 cation pumps on the inhibitory population of a meso scale cortical model has also been demonstrated. The inherent charge balancing characteristic of optogenetic channels ensures the cortex is not damaged by a transfer of charge between the extra-cellular space and the neurons. For an expression density of 10^9 ChR2's/m^2, we used a constant illumination intensity of 20 mW/mm^2 and a pulsed illumination intensity of 40 mW/mm^2 to push the seizing cortex away from seizure. The difference in intensities to produce similar results can be explained by the differences in the conductance profiles. While the conductance produced by a constant illumination profile is dependent only on the mean soma potential of the neuron population, the conductance produced by a pulsing light source depends on the variable illumination as well. In both cases, however, seizure waves were successfully inhibited.

Finally, to study the robustness of the control model to changes in the parameters in the model, we changed the strength of stochastic inputs, the neurotransmitter rate constants and the number of long range connections between cell populations, and changed the area of illuminated surface to account for the gyri and sulci in a cortex. Optogenetic control applied using constant illumination of different intensities successfully inhibited seizures in each case. It was also shown that while using pulsed illumination, the duration of time for which the cortex was not illuminated in between pulses played an important role in the behaviour of a seizing cortex. If the dark period was too long, weak synchronicity or seizure waves propagating at lower frequencies were produced.

To obtain an understanding of the dynamical system characterised by the cortical model coupled with the optogenetic model, we used AUTO (continuation and bifurcation software for ODEs) to study the nature of the dynamical changes wrought by variations in the model, as follows. By switching off the stochastic terms and the spatial terms in the PDEs, we obtain a set of ordinary differential equations (ODEs). P_{ee}, which is related to the excitation of the model, was varied to drive the cortex from normal function to seizure state resulting in the destabilising of the base state [9] engendering seizure dynamics. We restart the analysis and vary the light intensity, thus applying control to the inhibitory population. As the intensity is increased from $0.01 mW/mm^2$ to $40 mW/mm^2$ the base state again becomes stable, which is associated with the vanishing of the seizure dynamics. Further analysis of the nature of bifurcations and stability of the fixed points will be taken up in future work.

While this study suggests the use of optogenetics to inhibit seizure waves is possible, there are a number of improvements that can be made. The light cone produced by a light source will render variable illumination in the spatial domain [2]. This can be exploited for better spatial and temporal control of the activation of optogenetic channels. Also, incorporating a feedback loop will make this a more attractive control method because control can be applied only when seizure waves are detected.

Acknowledgements This work is partially supported by the US National Science Foundation grant CMMI 1031811.

References

1. Bojak, I., Liley, D.T.J.: Modeling the effects of anesthesia on the electroencephalogram. Physical Review E **71**, 041902 (2005)
2. Cardin, J., Carlén, M., Meletis, K., Knoblich, U., Zhang, F., Deisseroth, K., Tsai, L.H., Moore, C.: Targeted optogenetic stimulation and recordings of neurons *in vivo* using cell type specific expression of channelrhodopsin-2. Nature Protocols **5(2)**, 247–254 (2010)
3. Crick, F.: The impact of molecular biology on neuroscience. Physical Transactions of the Royal Society B: Biological Sciences **354**, 2021–2025 (1999)
4. Deisseroth, K.: Optogenetics. Nature Methods **8**, 26–29 (2011)
5. Gluckman, B., Nguyen, H., Weinstein, S., Schiff, S.: Adaptive electric field control of epileptic seizures. Journal of Neuroscience **21(2)**, 590–600 (2001)
6. Grossman, N., Nikolic, K., Toumazou, C., Degenaar, P.: Modeling study of the light stimulation of a neuron cell with channelrhodopsin-2 mutants. IEEE Transactions on Biomedical Engineering **58(6)**, 1742–1751 (2011)
7. Hegemann, P., Ehlenbeck, S., Gradmann, D.: Multiple photocycles of channelrhodopsin. Biophysical Journal **89**, 3911–3918 (2005)
8. Kramer, M., Kirsch, H., Szeri, A.J.: Pathological pattern formation and cortical propagation of epileptic seizures. Journal of the Royal Society Interface **2**, 113–127 (2005)
9. Kramer, M., Szeri, A., Sleigh, J., Kirsch, H.: Mechanisms of seizure propagation in a cortical model. Journal of Computational Neuroscience **22(1)**, 63–80 (2007)
10. Krook-Magnuson, E., Armstrong, C., Oijala, M., Soltesz, I.: On-demand optogenetic control of spontaneous seizures in temporal lobe epilepsy. Nature Communications **4:1376**, 1–8 (2013)
11. Liley, D.T.J., Cadusch, P.J., Dafilis, M.P.: A spatially continuous mean field theory of electrocortical activity. Network: Computation in Neural Systems **13**, 67–113 (2001)

12. Lopour, B.A., Szeri, A.J.: A model of feedback control for the charge-balanced suppression of epileptic seizures. Journal of Computational Neuroscience **28**, 375–387 (2010)
13. Nagel, G., Szellas, T., Huhn, W., Kateriya, S., Adeishvili, N., Berthold, P., Ollig, D., Hegemann, P., Bamberg, E.: Channelrhodopsin-2, a directly light-gated cation-selective membrane channel. Proceedings of the National Academy of Sciences **100(24)**, 13,940–13,945 (2003)
14. Paz, T.P., Davidson, T.J., Frechette, E.S., Delord, B., Parada, I., Peng, K., Deisseroth, K., Huguenard, J.R.: Closed-loop optogenetic control of thalamus as a tool for interrupting seizures after cortical injury. Nature Neuroscience **16**, 64-70 (2013)
15. Richardson, K., Schiff, S., Gluckman, B.: Control of travelling waves in mammalian cortex. Physical Review Letters **94**, 028,103 (2005)
16. Steyn-Ross, M.L., Steyn-Ross, D.A., Wilson, M.T., Sleigh, J.W.: Gap junctions mediate large-scale turing structures in a mean-field cortex driven by subcortical noise. Physical Review E **76**, 011,916 (2007)
17. Tønnesen, J., Sørensen, A., Deisseroth, K., Lundberg, C., Kokaia, M.: Optogenetic control of epileptiform activity. Proceedings of the National Academy of Sciences, USA **106**, 12,162–12,167 (2009)
18. Ursino, M., LaCara, G.E.: Travelling waves and EEG patterns during epileptic seizure: Analysis with an integrate-and-fire neural network. Journal of Theoretical Biology **242** (2006)
19. Zhang, F., Wang, L.P., Brauner, M., Liewald, J.F., Kay, K., Watzke, N., Wood, P.G., Bamberg, E., Nagel, G., Gottschalk, A., Deisseroth, K.: Multimodal fast optical interrogation of neural circuitry. Nature **446**, 633–641 (2007)